Supplemental Materials: Contrasting Transport Performance of Electron- and Hole-Doped Epitaxial Graphene for Quantum Resistance Metrology

Xinyi Wan(万歆祎)[1,2,3], Xiaodong Fan(范晓东)[1,2,3]**, Changwei Zhai(翟昌伟)[4,5], Zhenyu Yang(杨镇宇)[4,5], Lilong Hao(郝立龙)[1,2,3], Lin Li(李林)[1,2,3]**, Yunfeng Lu(鲁云峰)[4,5], and Changgan Zeng(曾长淦)[1,2,3]**

[1] *CAS Key Laboratory of Strongly Coupled Quantum Matter Physics, and Department of Physics, University of Science and Technology of China, Hefei 230026, China*

[2] *International Center for Quantum Design of Functional Materials (ICQD), Hefei National Research Center for Physical Sciences at the Microscale, University of Science and Technology of China, Hefei 230026, China*

[3] *Hefei National Laboratory, University of Science and Technology of China, Hefei 230088, China*

[4] *National Institute of Metrology, Beijing 100029, China*

[5] *Key Laboratory of Electrical Quantum Standards for State Market Regulation, Beijing 100029, China*

*Supported by the CAS Project for Young Scientists in Basic Research (Grant No. YSBR-046), the National Natural Science Foundation of China (Grant Nos. 92165201, 11974324, and 12104435), the Innovation Program for Quantum Science and Technology (Grant No. 2021ZD0302800), the Anhui Initiative in Quantum Information Technologies (Grant No. AHY170000), Hefei Science Center CAS (Grant No. 2020HSC-UE014), and the Fundamental Research Funds for the Central Universities (Grant Nos. WK3510000013 and WK2310000104). L.L. was also supported by USTC Tang Scholar. Part of this work was carried out at the Center for Micro- and Nanoscale Research and Fabrication, University of Science and Technology of China

** Email: fanxd@ustc.edu.cn; lilin@ustc.edu.cn; cgzeng@ustc.edu.cn

Text I: Fittings of the low-field magnetoconductivity data

The low field magnetoconductivity curves for n- and p-type devices were fitted using the following formula that is widely used to describe the weak localization effect in graphene, [1]

$$\Delta\sigma(B) = \frac{e^2}{\pi h}\left[F\left(\frac{B}{B_\phi}\right) - F\left(\frac{B}{B_\phi+2B_i}\right) - 2F\left(\frac{B}{B_\phi+B_i+B_*}\right)\right] \tag{S1}$$

where $F(z) = \ln z + \psi(1/2 + 1/z)$, $\psi(x)$ is the digamma function, $B_{\phi,i,*} = \hbar/(4De)\tau^{-1}_{\phi,i,*}$, D is the diffusion coefficient, and the characteristic scattering lengths are defined by $L_{\phi,i,*} = (D\tau_{\phi,i,*})^{1/2}$. As demonstrated in Fig. 3 and Fig. S4, all the data can be well fitted, and the values of L_ϕ can be extracted accordingly.

Text II: Estimation of the localization length

Fig. S5 further plots the conductance at 6 T as a function of temperature for two typical SiC/graphene devices (see Fig. 4 in the main text). It is clear that both the devices obey a well-defined variable range hopping (VRH) behavior of graphene, since the data can be well fitted via $\sigma_{xx} \propto \exp\left(-A/T^{1/2}\right)$, where $A = (4\hbar v_F/k_B\xi)^{1/2}$, v_F is Fermi velocity, k_B is the Boltzmann constant, ξ is localization length.[2] The extracted ξ for the n- and p-type devices are 30 nm and 97 nm, respectively.

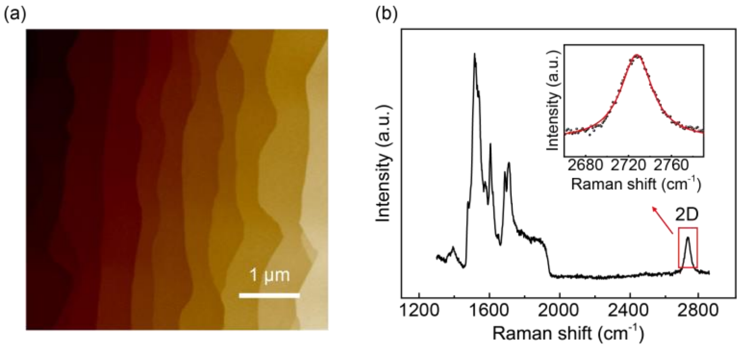

Figure S1: Basic characterizations of SiC/graphene samples. (a) Typical atomic force microscopy image of a SiC/graphene sample, from which clear terrace morphology is seen. (b) Raman spectrum of a SiC/graphene sample. The full width at half maximum of the 2D peak is approximately 36 cm^{-1}, indicating that the graphene is primarily composed of a single layer.[3,4] Inset: enlarged view of the 2D peak with a single Lorentzian fitting.

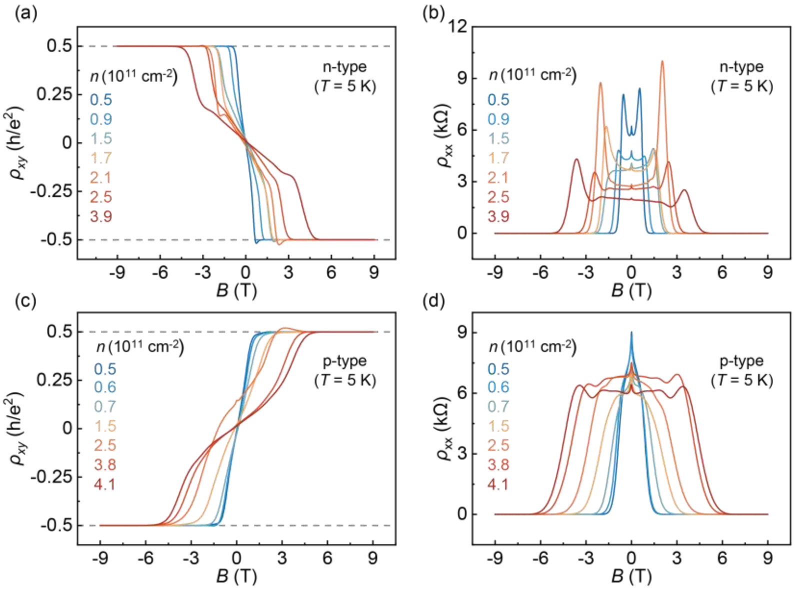

Figure S2: Raw data of the magneto-transport measurements at 5 K for various devices. [(a), (b)] Magnetic field dependence of (a) Hall resistivity ρ_{xy} and (b) longitudinal resistivity ρ_{xx} for n-type devices with different carrier densities. [(c), (d)] Magnetic field dependence of (c) ρ_{xy} and (d) ρ_{xx} for p-type devices.

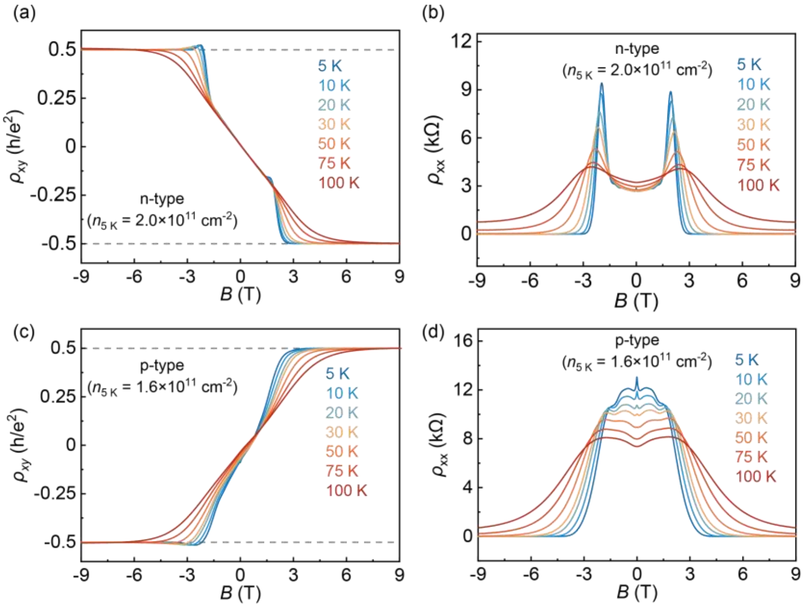

Figure S3: Raw data of the magneto-transport measurements conducted at different temperatures. [(a), (b)] Magnetic field dependence of (a) ρ_{xy} and (b) ρ_{xx} for a n-type device at various temperatures. [(c), (d)] Magnetic field dependence of (c) ρ_{xy} and (d) ρ_{xx} for a p-type device with similar carrier density.

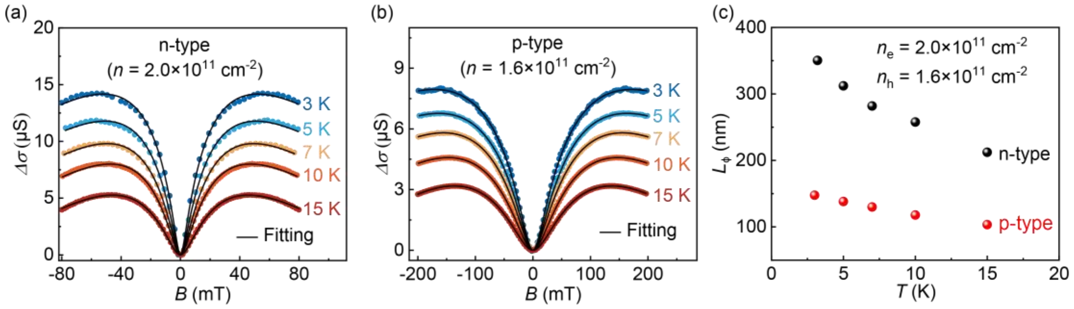

Figure S4: Fittings of the low-field magnetoconductivity data at various temperatures. [(a), (b)] Low-field magnetoconductivity data for (a) a n-type device and (b) a p-type one with similar carrier density. Here, $\Delta\sigma(B) = \sigma(B) - \sigma(0)$ corresponds to the change in conductivity relative to the zero-field value. The solid lines are fitting results using formula (S1). (c) The extracted values of phase coherence length at different temperatures for these two devices.

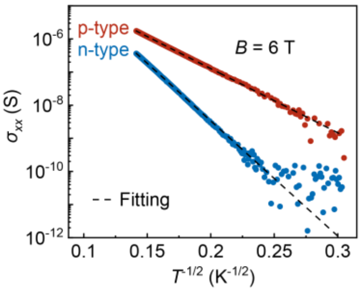

Figure S5: Estimation of the localization length based on the VRH mechanism. Conductance σ_{xx} vs $T^{-1/2}$ for the n- and p-type devices under a 6 T magnetic field, and the corresponding fitting results (black dashed lines).

References

[1] McCann E, Kechedzhi K, Fal'ko V I, Suzuura H, Ando T, and Altshuler B L 2006 *Phys. Rev. Lett.* **97** 146805

[2] Yang S J and Yu Y 2004 *Phys. Rev. B* **69** 233307

[3] Lee D S, Riedl C, Krauss B, von Klitzing K, Starke U, and Smet J 2008 *Nano Lett.* **8** 4320

[4] Giannazzo F, Deretzis I, La Magna A, Roccaforte F, and Yakimova R 2012 *Phys. Rev. B* **86** 235422